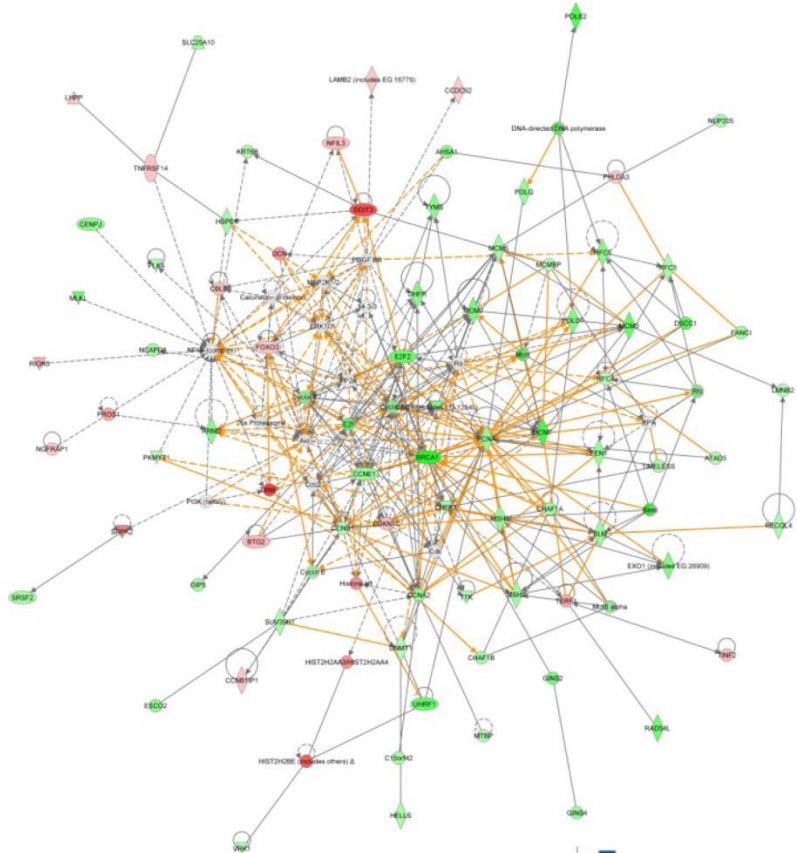


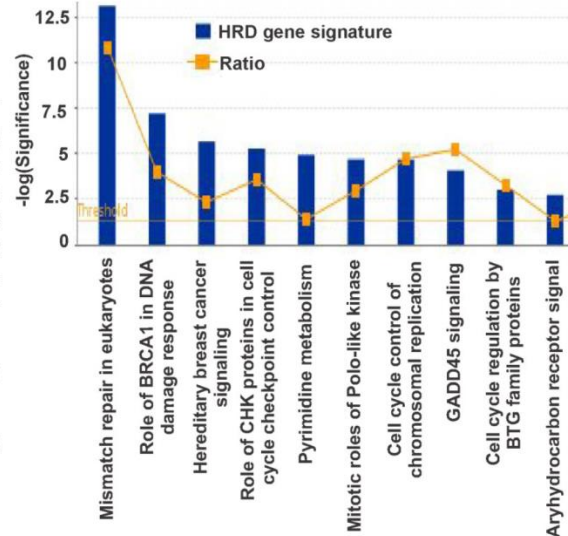
Supplementary Figure 1: Establish HRD cell lines to generate “the HRD gene signature”. (a) Schematic diagram of HR repair assay. The DRGFP reporter substrate was integrated into cellular genomic DNA. SceGFP contains an I-SceI endonuclease site within the coding region, which abolishes GFP expression. iGFP is a truncated GFP, which contains homologous sequence for the SceGFP. Expression of I-SceI induces a single DSB in the genome. When this DSB is repaired by HR, the expression of GFP can be restored and analyzed by flow cytometry to indicate the efficiency of HR repair. (b) MCF-10A cells were infected with lentiviral particles targeting *BRCA1*, *RAD51* or *BRIT1*. Selected stable clones were subject to HR repair assay as described above. Each value is relative to the percentage of GFP-positive (GFP+) cells in I-SceI-transfected control cells. Results are shown as mean + SD from three independent experiments; Student’s *t*-test was used to test statistical significance. (c) Whole cell lysate was analyzed by western blotting via indicated antibodies, demonstrating effective knockdown by shRNA (target sequences in Supplementary Table 3). Flow cytometry analyses of cell cycle distribution in these cell lines were shown next to Western blots.

a**b****Molecular and Cellular Functions**

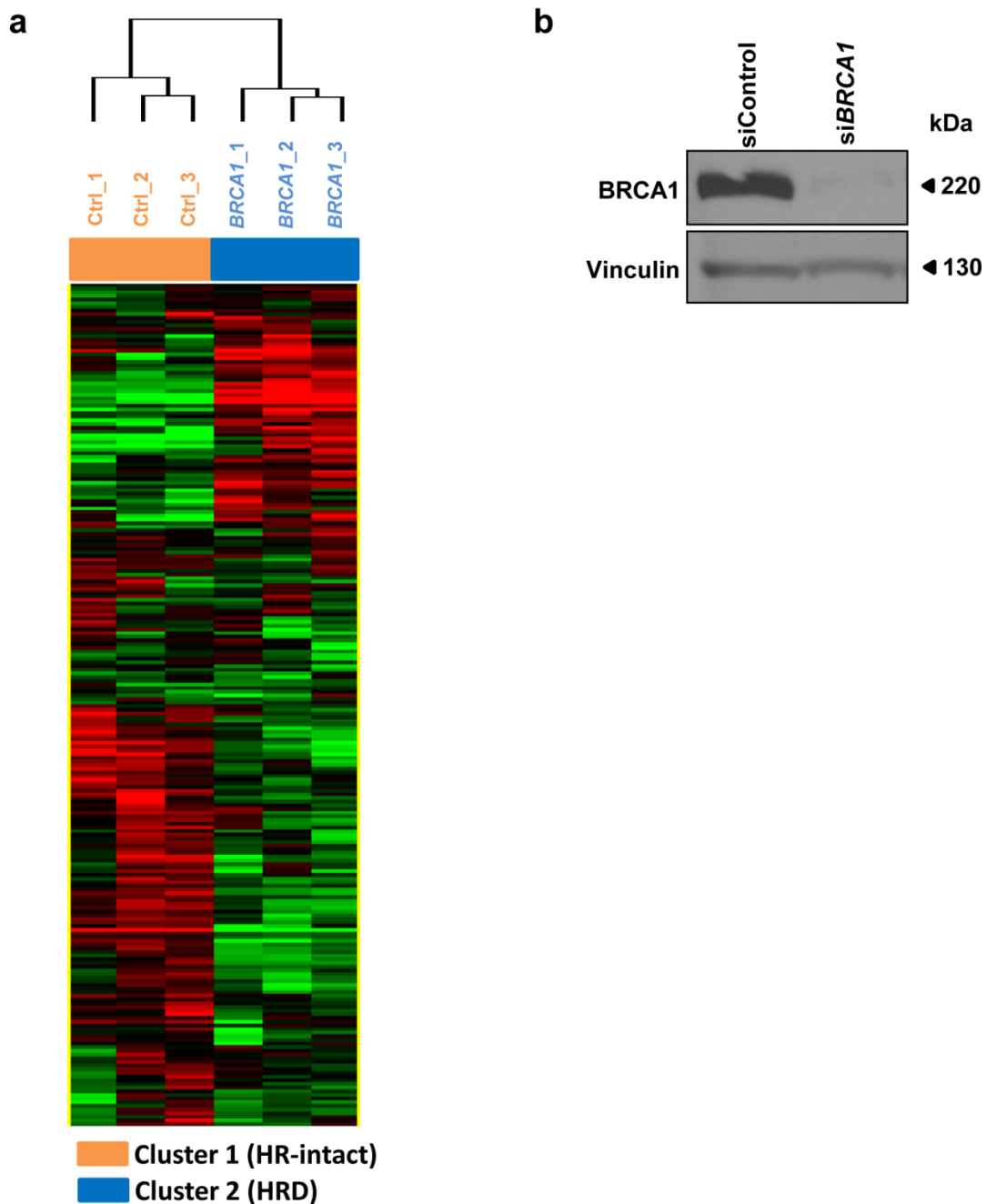
Name	p-value	#Molecules
Cell Cycle	6.87E-13-1.94E-02	68
DNA Replication, Recombination, and Repair	2.06E-11-1.74E-02	69
Cellular Assembly and Organization	8.93E-10-1.73E-02	46
Cellular Function and Maintenance	1.24E-07-1.94E-02	28
Cell Death	7.87E-04-1.94E-02	79

Top Canonical Pathways

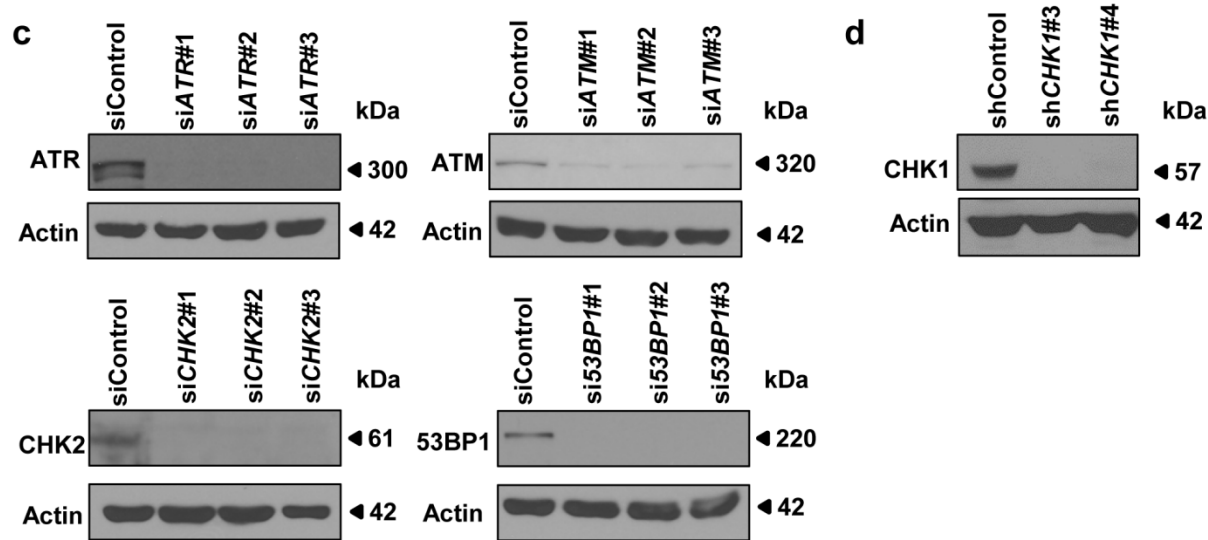
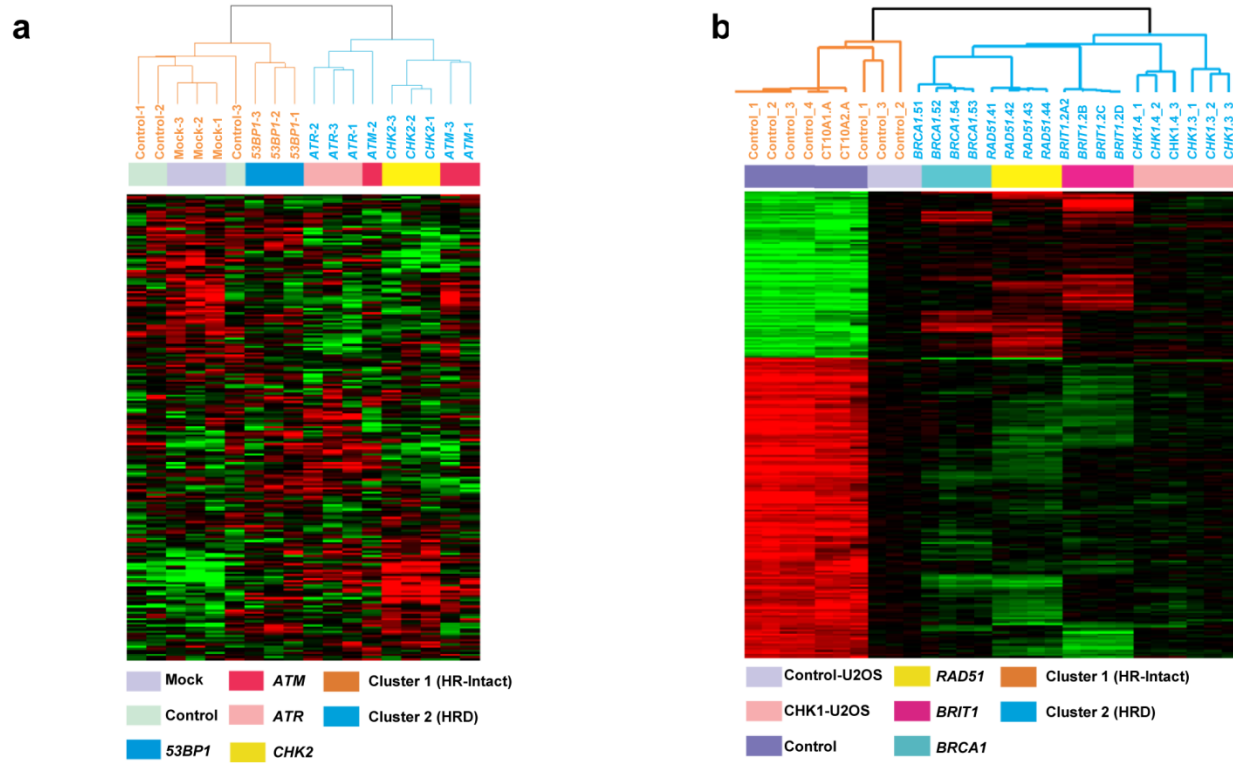
Name	p-value	Ratio
Mismatch Repair in Eukaryotes	7.92E-14	9/24 (0.375)
Role of BRCA1 in DNA Damage Response	6.30E-08	9/65(0.138)
Hereditary Breast Cancer Signaling	2.13E-06	10/127(0.079)
Role of CHK Proteins in Cell Cycle Checkpoint Control	5.29E-06	7/56(0.125)
Pyrimidine Metabolism	1.17E-05	10/215(0.047)



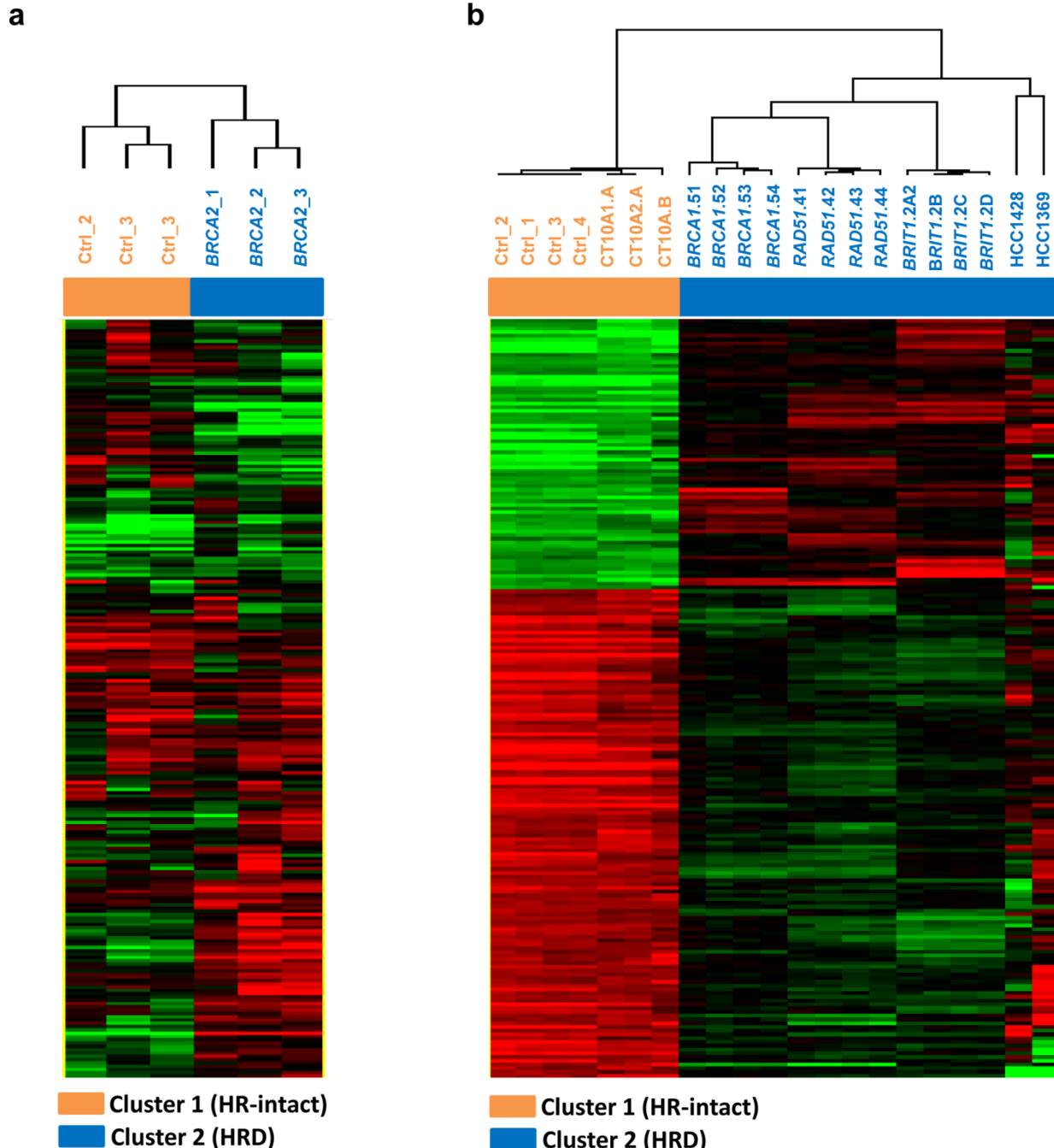
Supplementary Figure 2: Genes in the HRD gene signature are involved in various cellular processes. (a) The networks with the largest numbers of genes in the HRD gene signature on analysis with Ingenuity Systems' IPA software were cell cycle; DNA replication, recombination, and repair; and cellular assembly and organization. Red nodes, up-regulated genes; green nodes, down-regulated genes. (b) Top ten canonical pathways in terms of number of genes in the HRD gene signature on analysis with Ingenuity Systems' IPA software. Significance refers to the $-\log(p\text{ value})$, which is obtained by the Ingenuity program using Fisher's exact test. Threshold is at $P=0.05$.



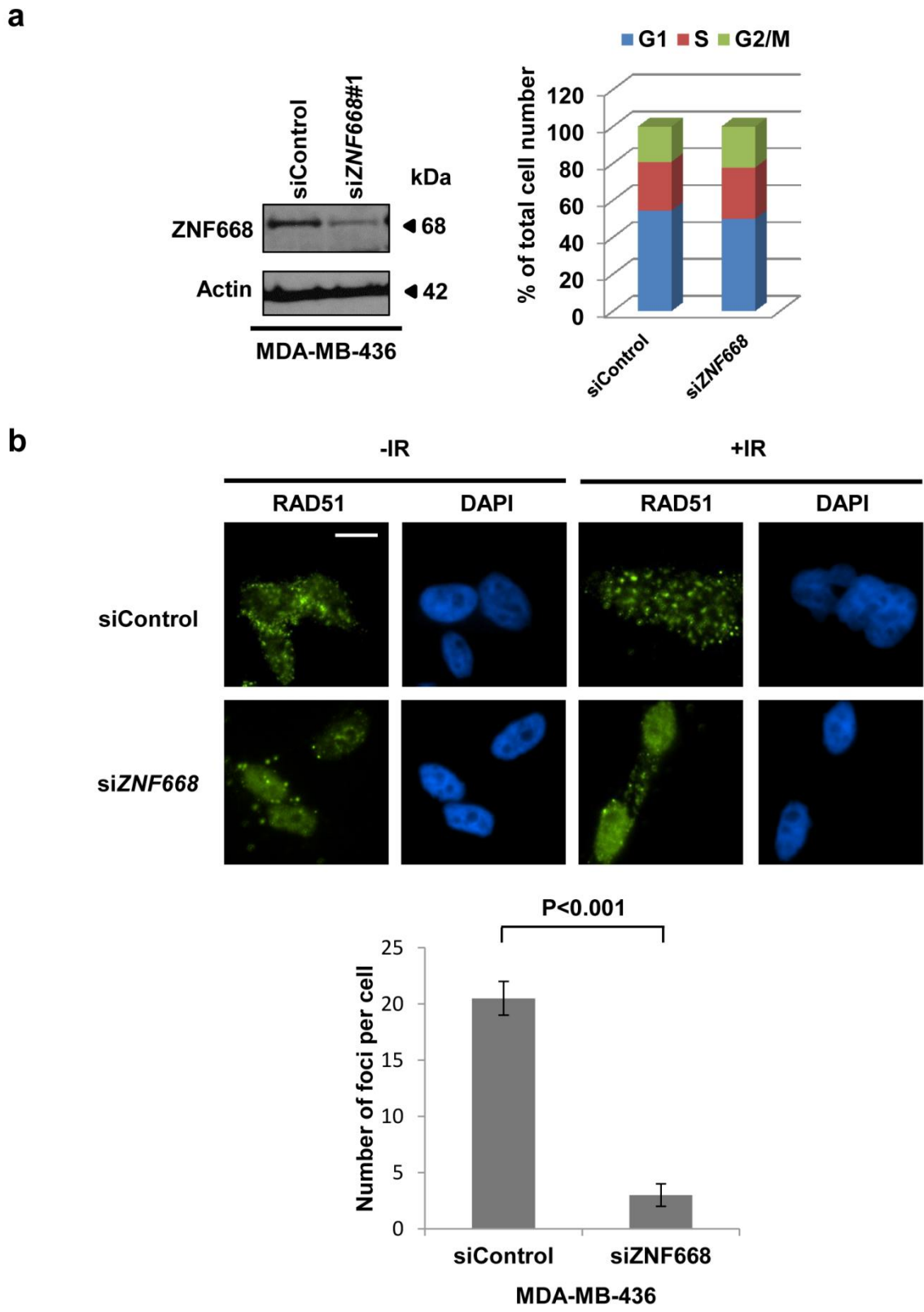
Supplementary Figure 3: Transient siRNA knockdown *BRCA1* also reveals HRD gene signature. (a) MCF-10A cells were transfected with siRNA targeting *BRCA1*. Microarray analyses were conducted to verify accuracy and specificity of the HRD gene signature by supervised clustering analysis. (b) Western blot analyses demonstrated effective knockdown.

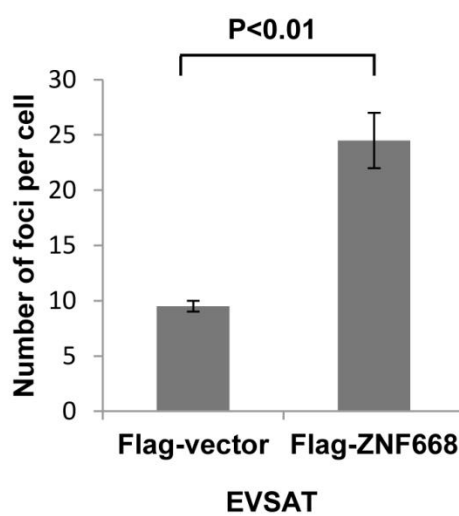
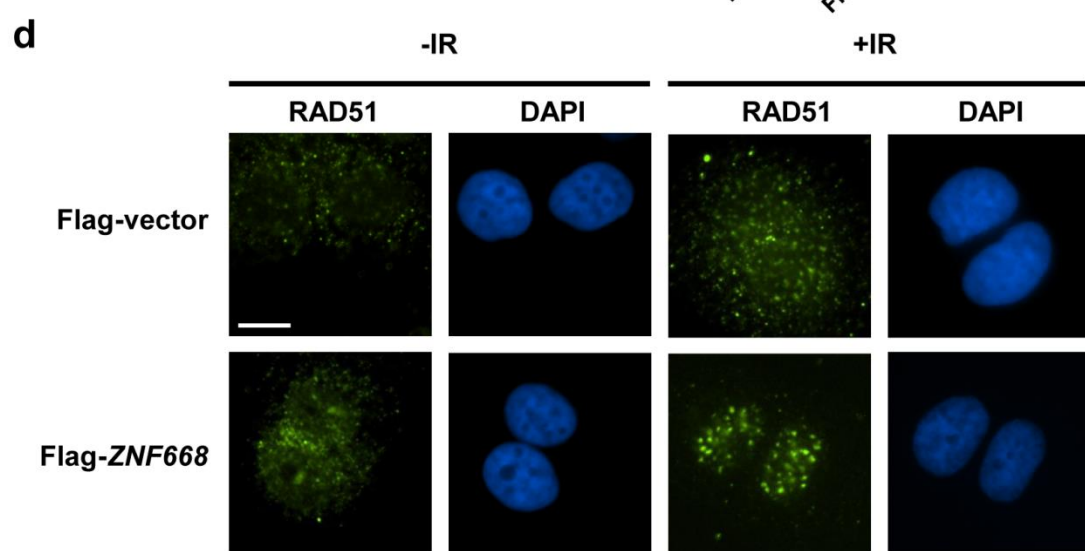
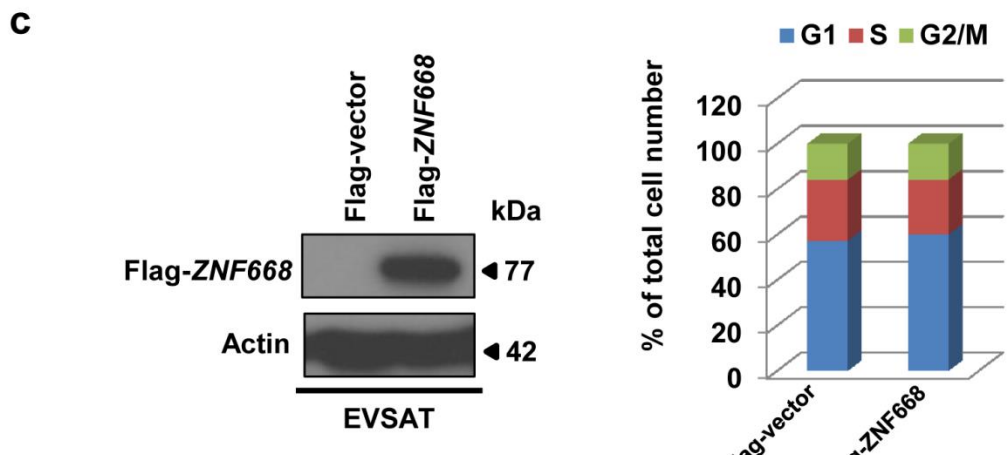


Supplementary Figure 4: The HRD gene signature predicts HRD induced by knockdown of different HR-related genes. (a) MCF-10A cells were transiently transfected with siRNAs targeting *ATM*, *ATR*, *CHK2*, or *53BP1*, and (b) U2OS cells were infected by lentiviral particles targeting *CHK1*. Microarray analyses were conducted to verify accuracy and specificity of the HRD gene signature by supervised clustering analysis. (c and d) Western blot analyses demonstrated effective knockdown.



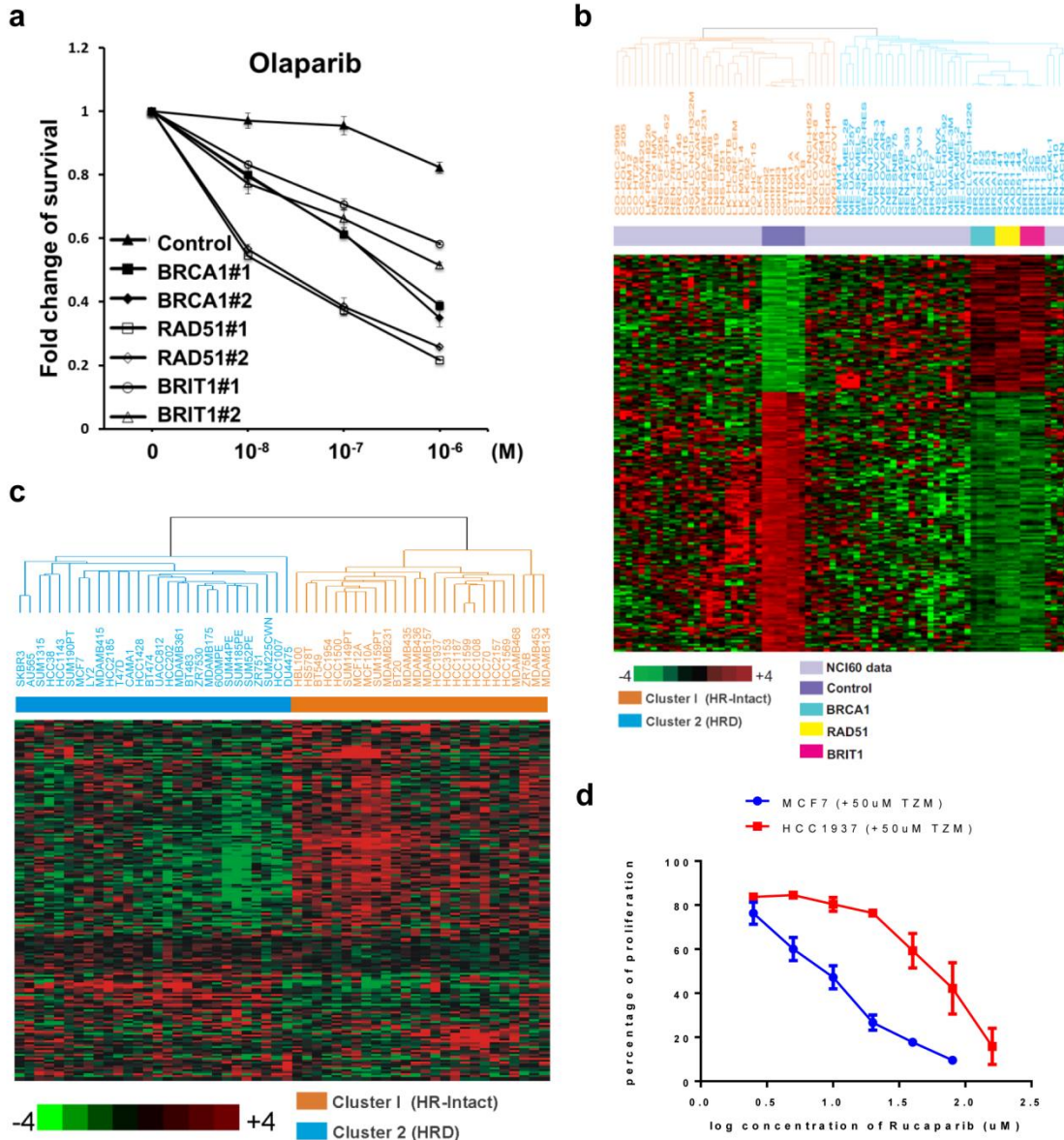
Supplementary Figure 5: Cells with *BRCA2* deficiency displays HRD signature. (a) MCF-10A cells were transfected with shRNA targeting *BRCA2*. Microarray analyses were conducted to verify accuracy and specificity of the HRD gene signature by supervised clustering analysis. (b) Two *BRCA2* defective breast cancer cell lines were selected for supervised clustering analysis with HRD gene signature. HCC1428 has 6174delT mutation resulting in a 2135-base-pair deletion. HCC1369 has a nonsense mutation that causes protein truncated at E1593.



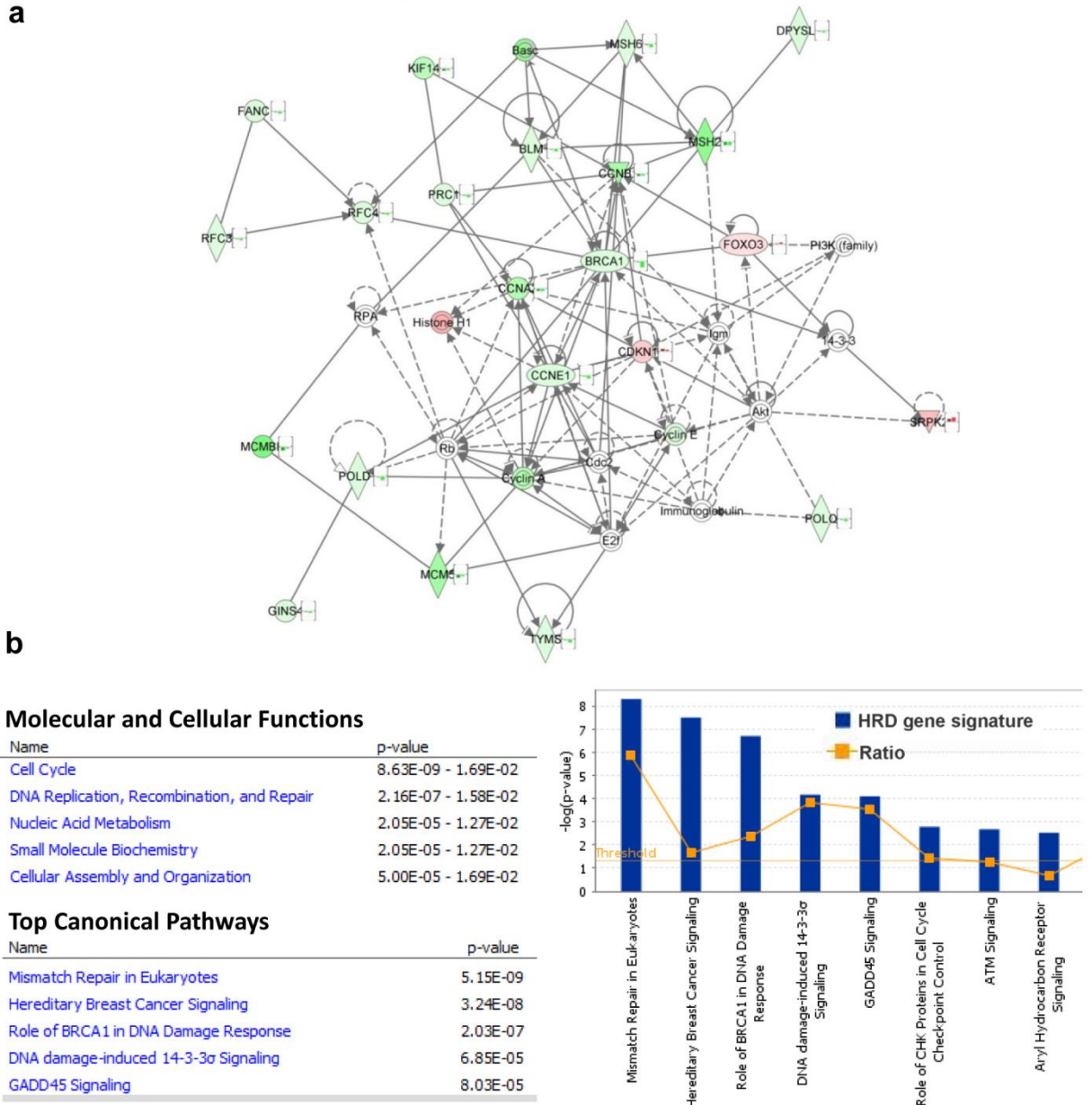


Supplementary Figure 6: Depletion of ZNF668 significantly reduces RAD51 foci formation, but does not affect cell cycle distribution. (a) MDA-MB-436 cells were transfected with control or ZNF668 siRNA. Left:

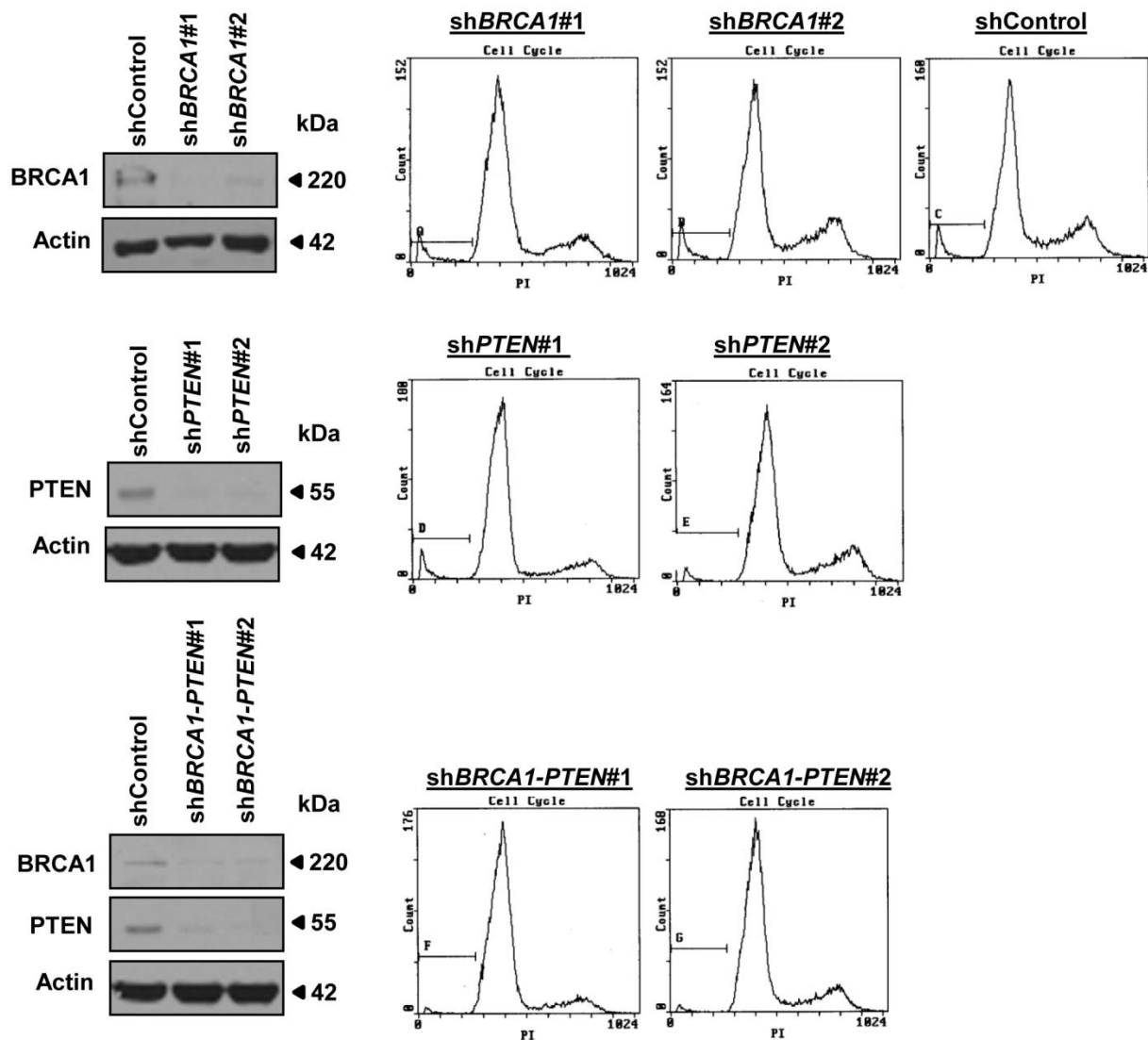
Effective knockdown are shown. Right: Cell cycle analysis seventy-two hours after transfection. **(b)** RAD51 foci formation in MDA-MB-436 cells transfected with control or *ZNF668* siRNA. Irradiated and nonirradiated cultures were stained with an anti-RAD51 pAb and foci were visualized by microscopy. Top: representative immunostaining images. Bottom: the bar graph is shown as the mean \pm SEM; Student's *t*-test. At least 50 cells were scored in each sample from three independent replications. Scale bar is 10 μ m. **(c)** EVSAT cells were transfected with Flag-vector or Flag-ZNF668. Left: Effective knockdown are shown. Right: Cell cycle analysis seventy-two hours after transfection. **(d)** RAD51 foci formation in EVSAT cells transfected with Flag-vector or Flag-ZNF668. Irradiated and nonirradiated cultures were stained with an anti-RAD51 pAb and foci were visualized by microscopy. Top: representative immunostaining images. Bottom: the bar graph is shown as the mean \pm SEM; Student's *t*-test. At least 50 cells were scored in each sample from three independent replications. Scale bar is 10 μ m.



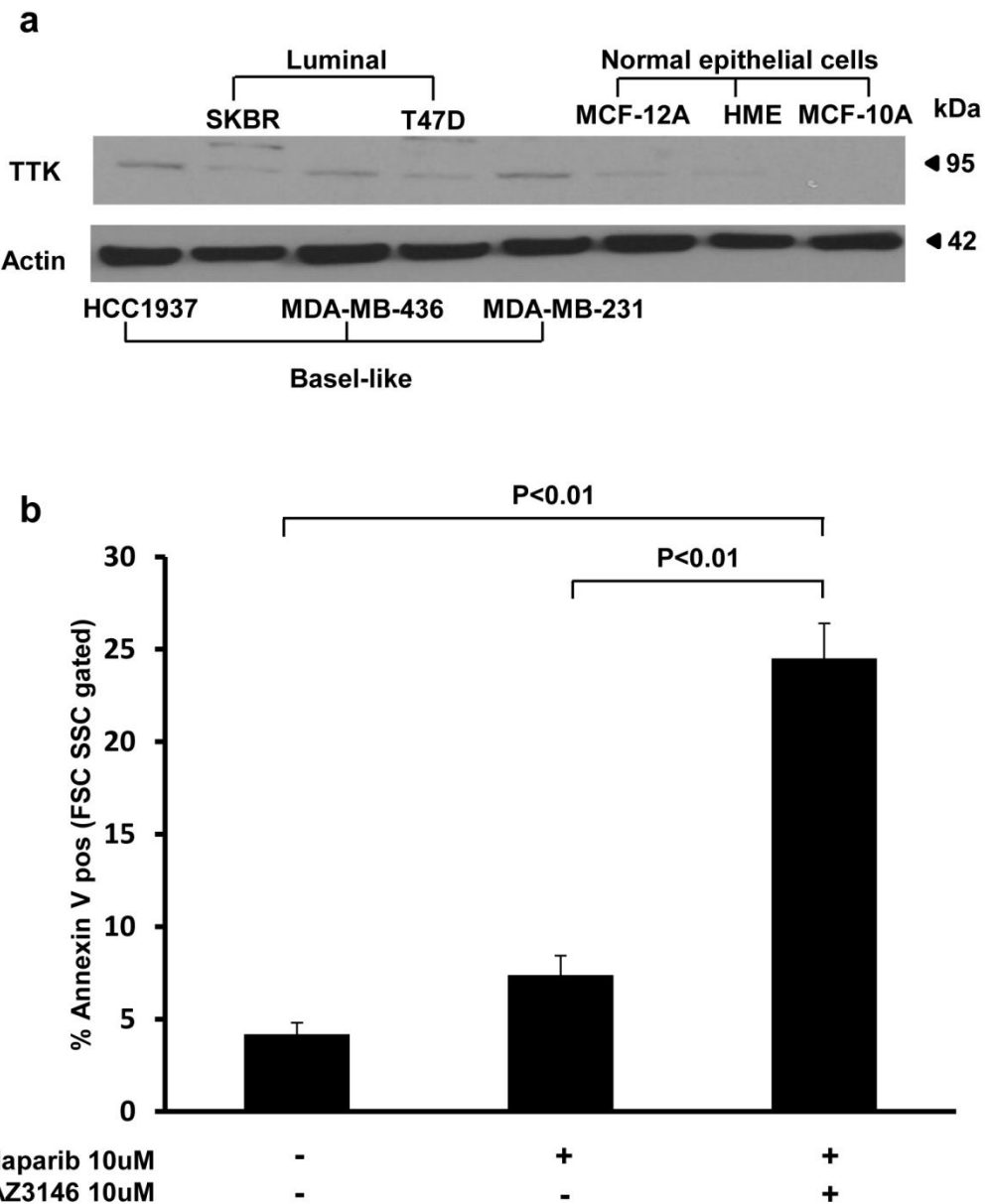
Supplementary Figure 7: The HRD Gene Signature Predicts HR-deficiency and Sensitivity to PARP Inhibitors in Cancer Cells. (a) Cells were seeded in a very low density and treated with indicated concentrations of PARP inhibitor olaparib for 10-15 days to allow colony formation. The rate of cell survival was determined by colony-formation assay. Colonies were stained with 0.25% crystal violet/25% methanol and counted both manually and digitally using ImageJ software. Each value was relative to control cells that contain only DMSO (solvent for olaparib) and represents the mean \pm SEM from three independent experiments. Student's *t*-test showed that the drug response to olaparib differed between control cell lines and individual knockdown cell lines ($P < 0.05$). (b) Microarray data from the NCI60 cell lines were analyzed by supervised clustering on the basis of the HRD gene signature. (c) Microarray data from 51 breast cancer cell lines were analyzed by supervised clustering on the basis of the HRD gene signature. HR-intact and HR-deficient cell lines were shown. (d) MTT assay was performed with indicated concentrations of rucaparib combined with 50 μ M of Temozolomide (TZM). Each value is relative to the value in the cells treated with vehicle control. Results are shown as mean \pm SEM from three independent experiments. Student's *t*-test showed that the drug response to rucaparib differed between cancer cell lines with and without the HRD gene signature ($P < 0.05$).



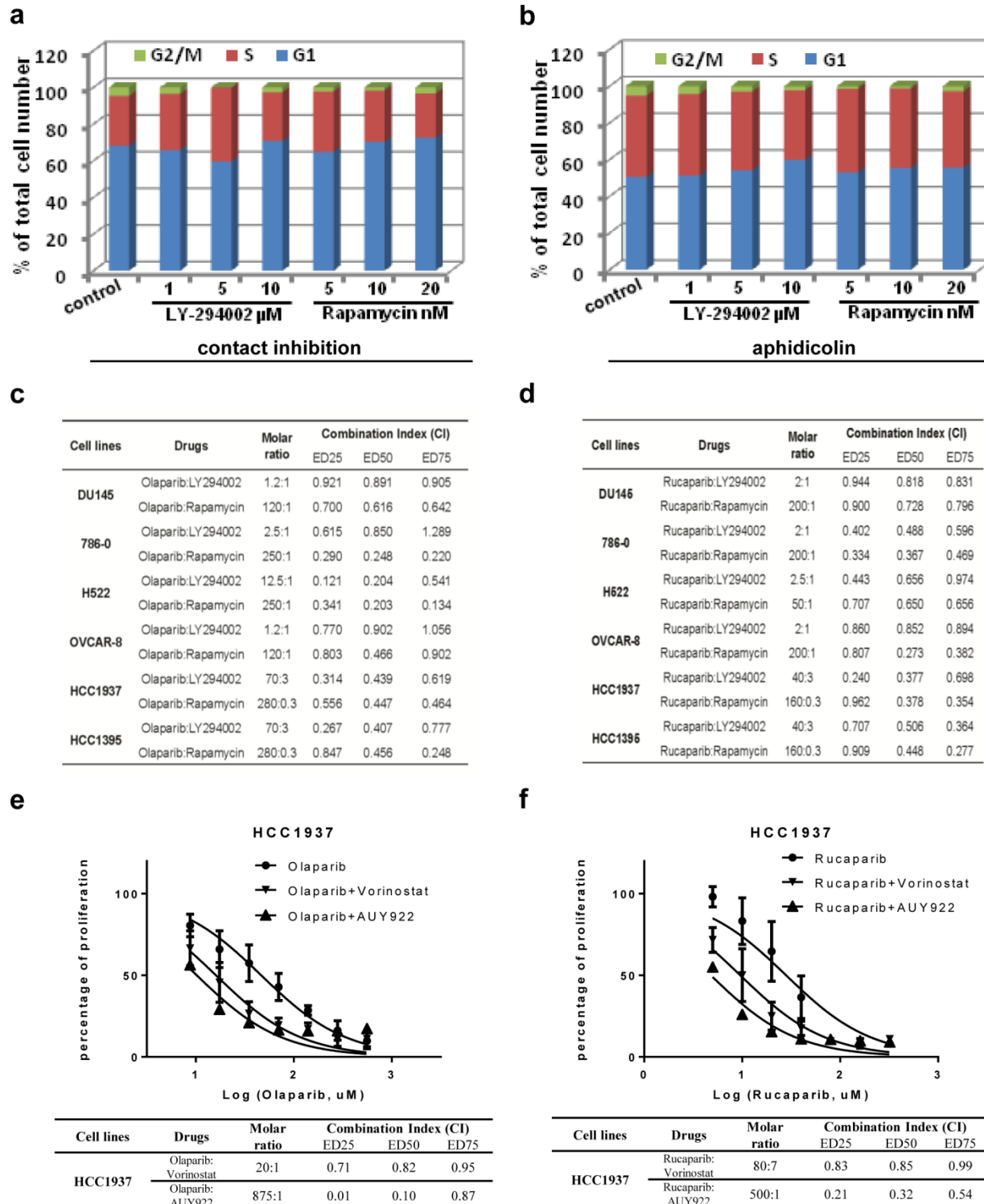
Supplementary Figure 8: The expression changes of HRD-associated protein are correlated with transcriptional alterations. (a) Both HRD gene and protein expressions are within the network of cell cycle; DNA replication, recombination, and repair; and cellular assembly and organization was analyzed by Ingenuity Systems' IPA software. In bar chat, left bar indicates gene expression changes and right bar indicates protein expression changes. Red nodes and bars indicates up-regulated genes or proteins and green nodes and bars indicates down-regulated genes or proteins.(b) Top canonical pathways in terms of number of genes in the HRD-associated proteins on analysis with Ingenuity Systems' IPA software. Significance refers to the $-\log(p\text{ value})$, which is obtained by the Ingenuity program using Fisher's exact test. Threshold is at $P=0.05$.



Supplementary Figure 9: Validation of effective *BRCA1* or *PTEN* single-gene-knockdown and *BRCA1-PTEN* double knockdown. MCF-10A cells were infected with lentiviral particles targeting *BRCA1*, *PTEN* or Both. Cells were selected in puromycin (1 μ g/mL) for 10-15 days and then subjected to western blotting, demonstrating effective knockdown by indicated antibodies. Cell cycle distribution in these cell lines were shown next to Western blots.

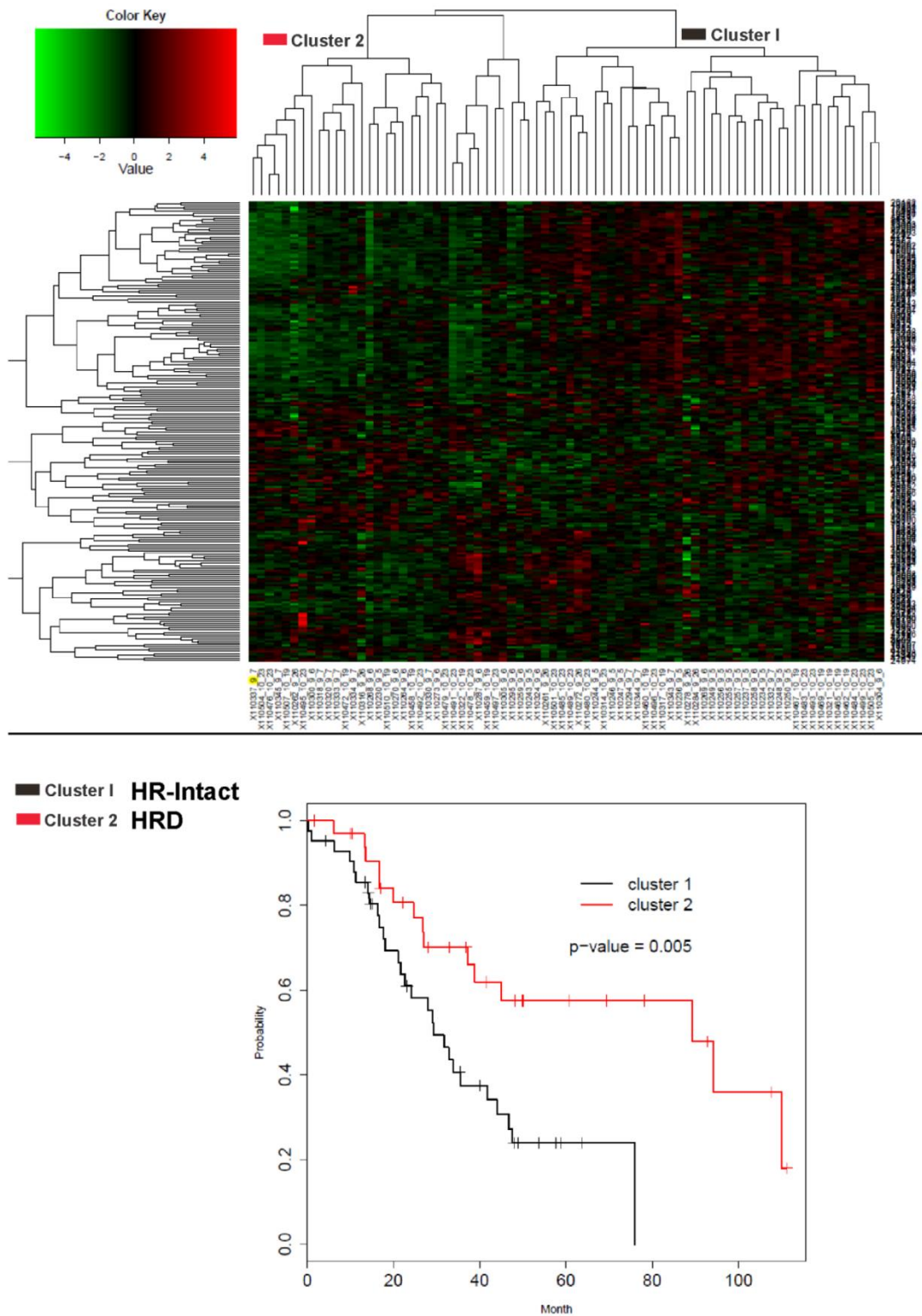


Supplementary Figure 10: TTK inhibitor enhances apoptosis induced by PARP inhibitor. (a) TTK expression levels in basal-like or luminal breast cancer cell lines and immortal human mammary epithelial cells. Cell lysates were harvested from indicated cell lines and subjected to western blotting analysis. (b) HCC1937 cells were treated with olaparib, or combined with TTK inhibitor AZ3146 for 48 hours and subjected to apoptosis analysis. Each value represents the mean + SD from three independent experiments. Student's *t*-test showed increased apoptosis led by olaparib combined with AZ3146 compared to control or olaparib alone ($P<0.01$).



Supplementary Figure 11: Validation of PARP-inhibitor-synergizing agents. (a) U2OS cells were seeded at a high density to allow contact inhibition and transfected with I-SceI plasmid to induce DSBs. Then cells were treated with the indicated concentrations of PI3K inhibitor LY-294002 or mTOR inhibitor rapamycin for 16 hr before flow cytometry analysis of cell cycle distribution. (b) U2OS cells were treated with the indicated concentrations of LY-294002 or rapamycin after I-SceI transfection and then treated with replication inhibitor aphidicoline (10 μ M) to

synchronize cell cycle for 16 hr before flow cytometry analysis of cell cycle distribution. (**c** and **d**) The indicated cancer cell lines were treated with single or combined treatment of PARP inhibitor olaparib (**c**) or rucaparib (**d**), with LY-294002 or rapamycin and analyzed by MTT assay. The CI values were calculated by CompuSyn software. (**e** and **f**) HCC1937 cells were treated with single or combinations of olaparib (**e**) or rucaparib (**f**) with HDAC inhibitor vorinostat or Hsp90 inhibitor AUY922 and analyzed by MTT assay. Each value is relative to the value in the cells treated with vehicle control (DMSO). Results are shown as mean \pm SEM from three independent experiments. The CI values calculated by CompuSyn software are listed at the bottom.



Supplementary Figure 12: The HRD Gene Signature Predicts Overall Survival in an Ovarian Cancer Patient Cohort. Datasets from patients with ovarian cancer were clustered into two groups on the basis of whether the gene expression pattern was similar to the HRD gene signature. Kaplan-Meier overall survival curves are shown. P values are from log-rank test.

Figure 1e

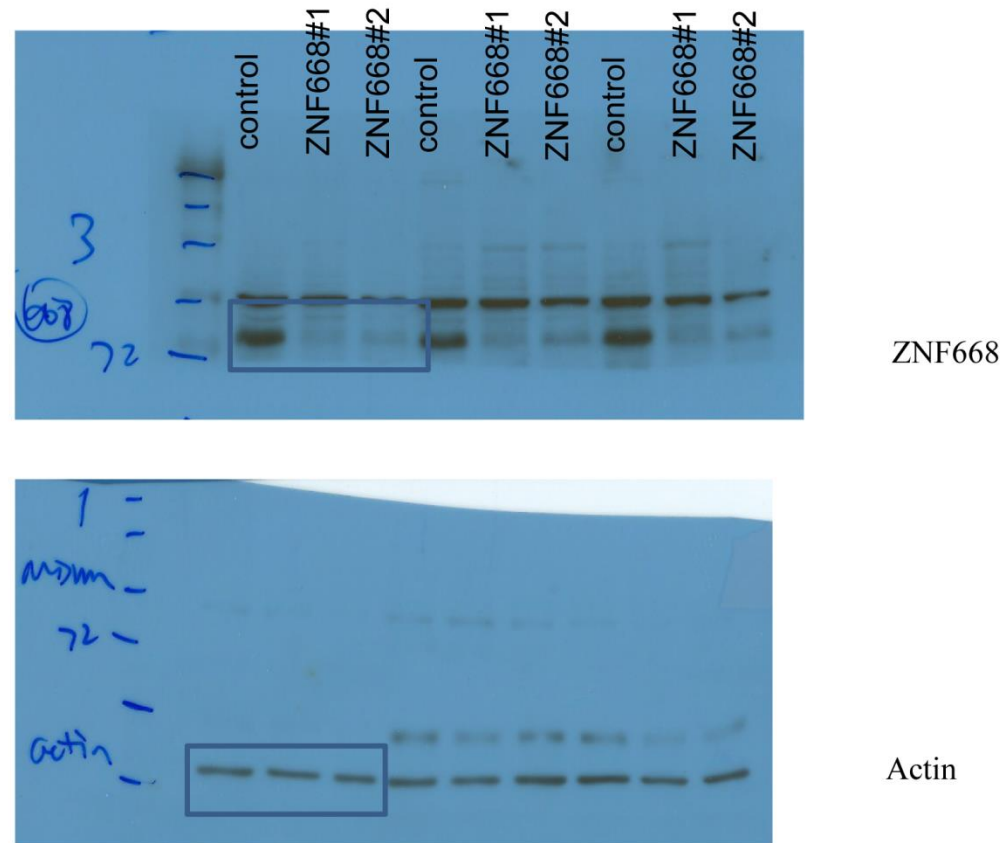
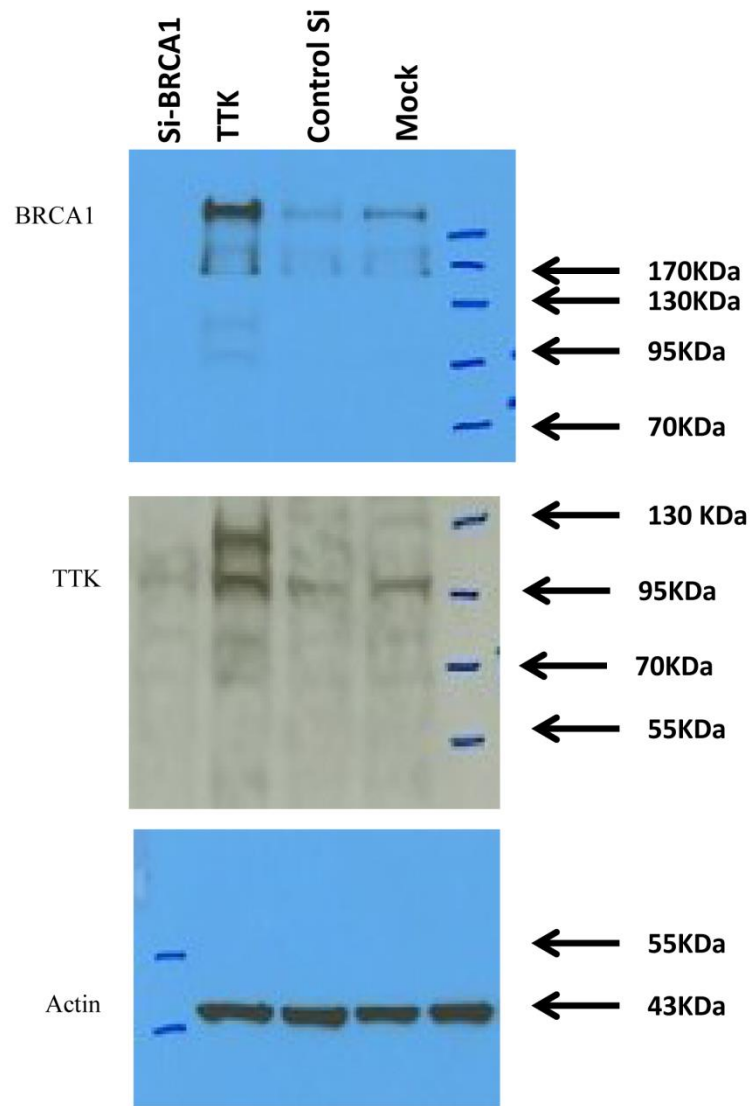
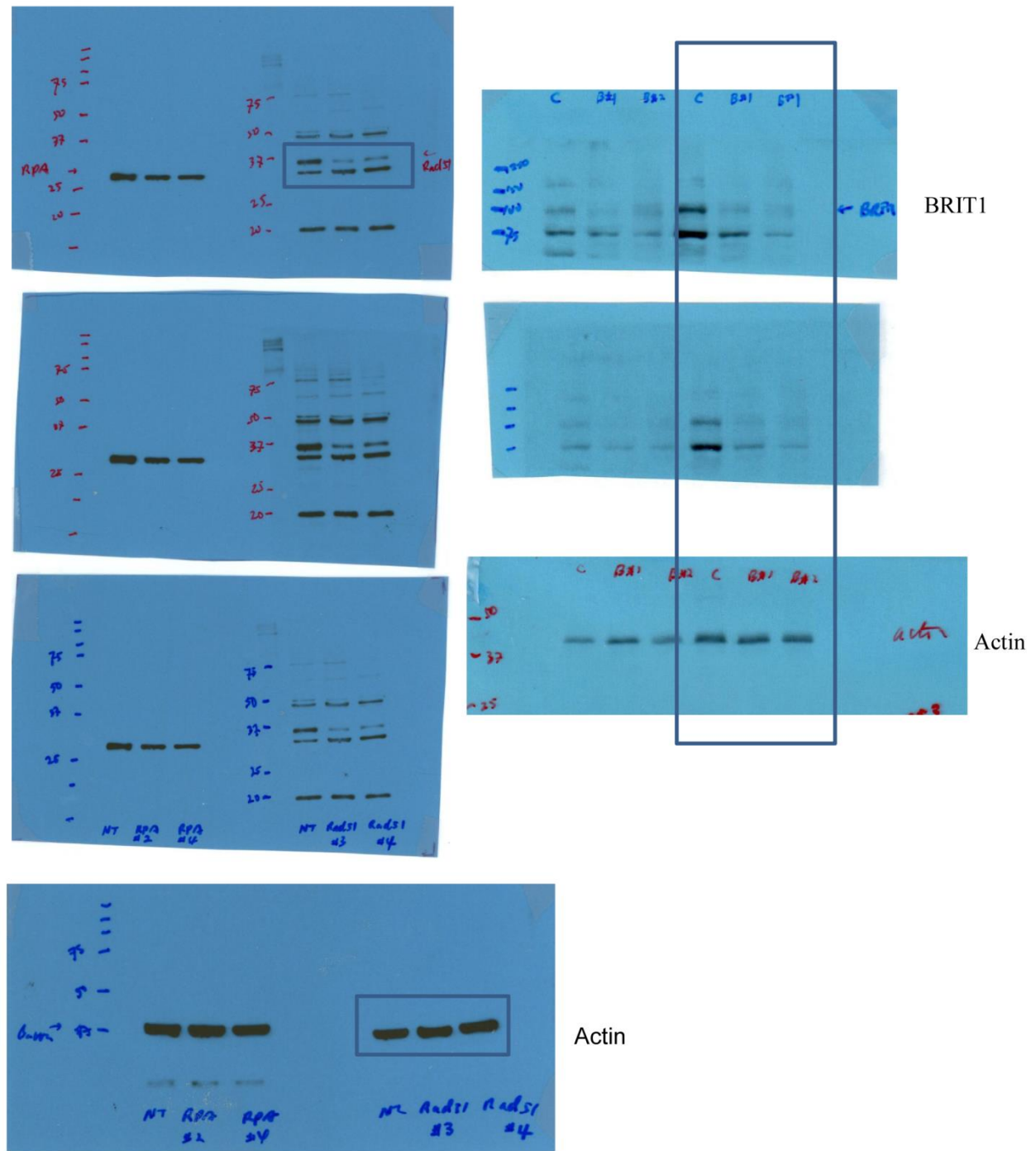


Figure 3f

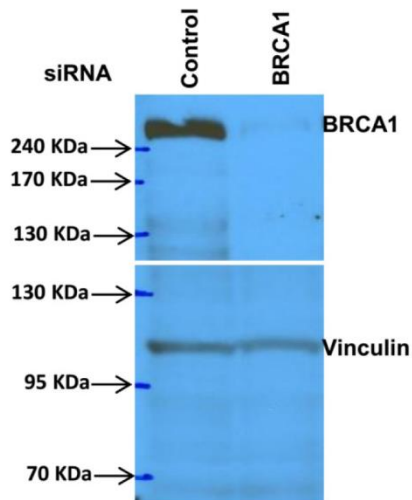


Supplementary figure 1c

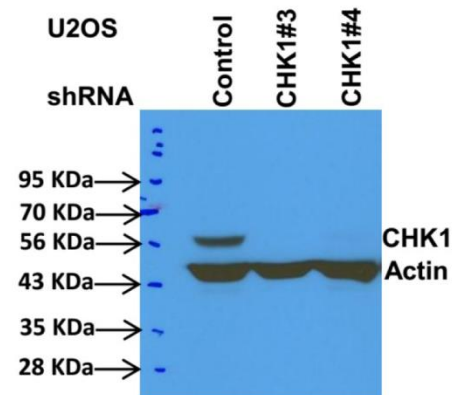
RAD51 different exposure time



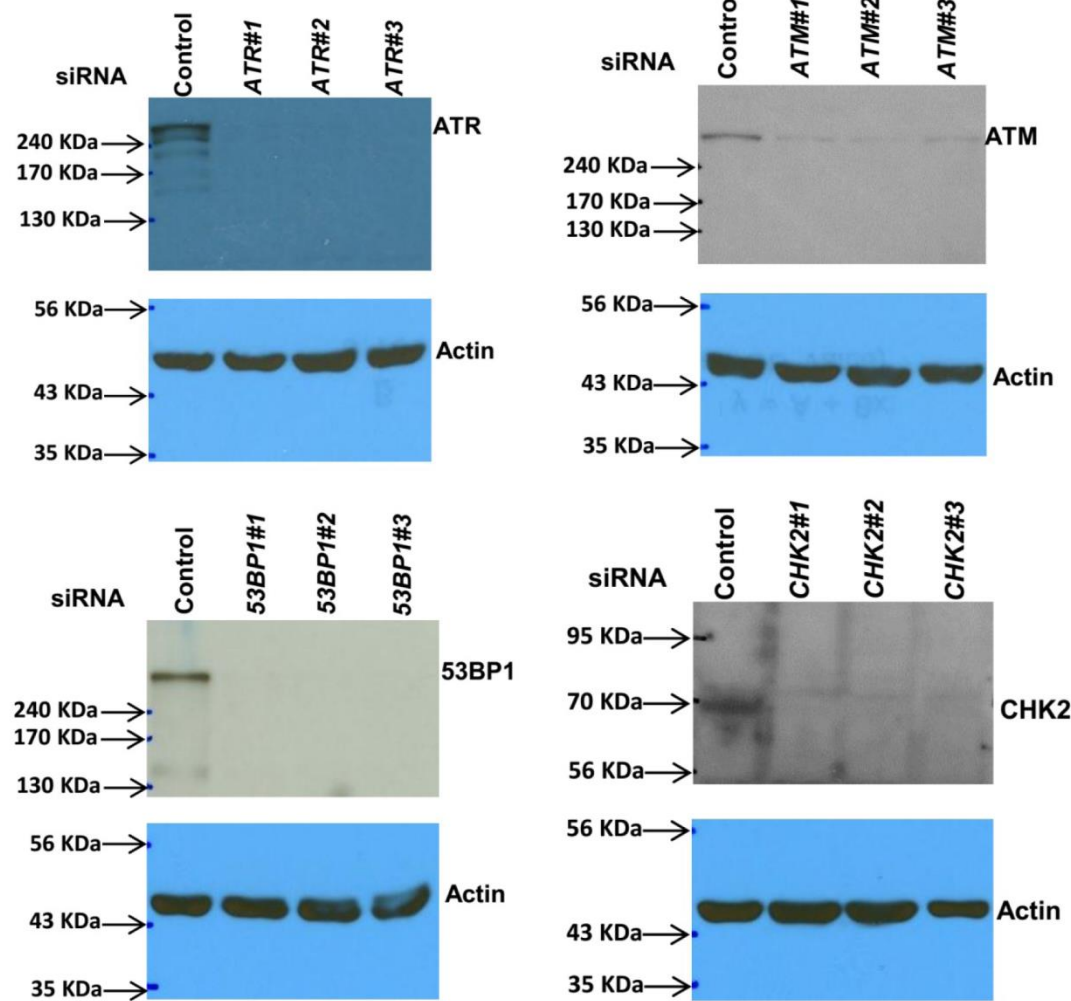
Supplementary figure 3b



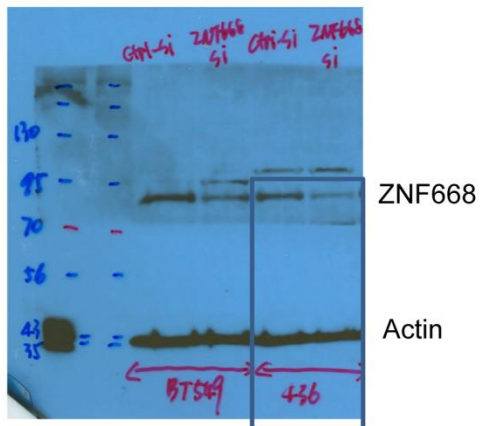
Supplementary figure 4d



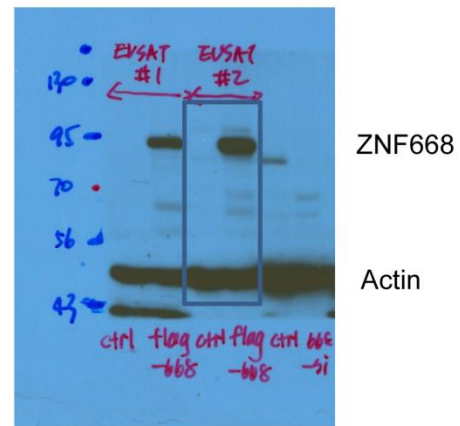
Supplementary figure 4c



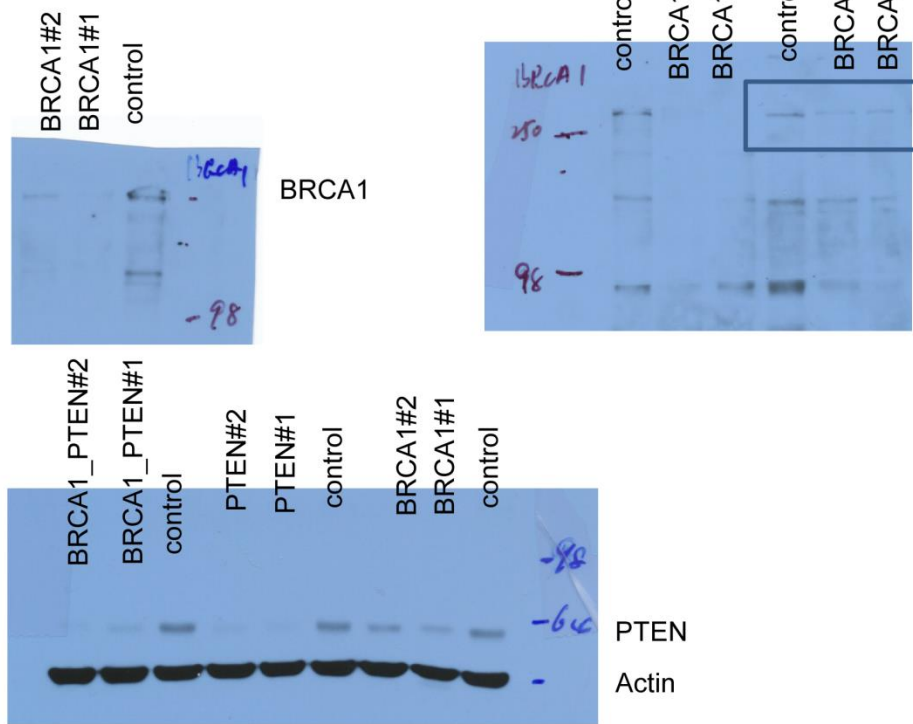
Supplementary figure 6a



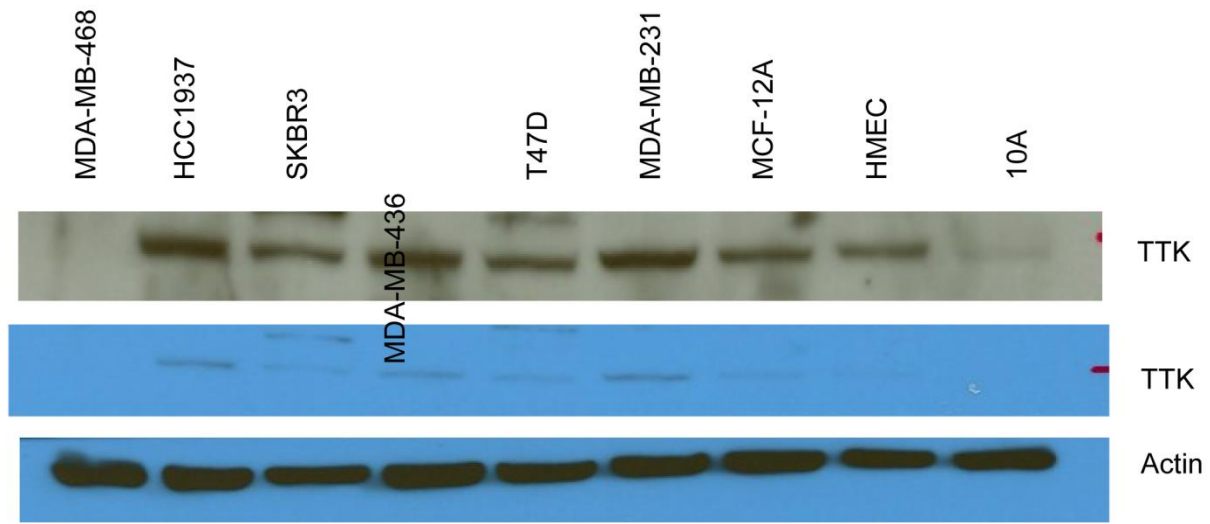
Supplementary figure 6c



Supplementary figure 9



Supplementary figure 10a



Supplementary Figure 13. Full western blots for the most important blots presented in the manuscript.

Supplementary Table 1: The list of 230 genes designated as “the HRD gene signature”

Gene Symbol	Gene expression of <i>BRCA1</i>-shRNA/Control-shRNA	Gene expression of <i>Rad51</i>-shRNA/Control-shRNA	Gene expression of <i>BRIT1</i>-shRNA/Control-shRNA
AADAT	0.471246673	0.427892763	0.432906783
ADM	3.507136497	5.103009422	2.790489783
AHSA1	0.291138066	0.461385918	0.296262701
ALDH3B1	5.644456865	3.777395591	7.888853059
ALDH6A1	3.236368847	3.79262783	5.167951941
ALG8	0.459931384	0.397772753	0.34249794
ANLN	0.220233364	0.323484705	0.208461603
ARSD	2.685153685	2.945231199	3.551956525
ASF1B	0.287942058	0.271904934	0.423418935
ASPM	0.443153553	0.340791181	0.293972923
ATP10B	11.45032332	2.619587325	2.807987684
AURKB	0.402971907	0.242753108	0.401651106
BBOX1	2.251985602	2.749547001	5.101010704
BLM	0.348773858	0.324850004	0.34527865
BRCA1	0.158563144	0.307140816	0.25875128
BRI3BP	0.284146678	0.251749729	0.201364129
BTG1	2.328370191	2.657785691	3.436277395
BTG2	2.834902128	4.627634029	2.640251946
C10orf119	0.484065665	0.419366671	0.379577859
C10orf73	2.86756586	2.580412469	3.010173261
C11orf82	0.473975374	0.286688513	0.183979576
C13orf3	0.445754679	0.3407389	0.327124395
C14orf145	0.460067907	0.417533953	0.474498081
C15orf42	0.40006462	0.354142825	0.467109046
C16orf59	0.387077719	0.308330282	0.348590363
C16orf68	2.03686802	2.268657709	2.100196149
C17orf41	0.455972071	0.437616789	0.378696917
C1orf112	0.420918188	0.262825244	0.324277978
C1orf54	2.086238116	2.331730985	2.204903467
C1QTNF6	0.371633949	0.472534482	0.467885864
C20orf19	3.47770913	5.518372187	2.553267054
C20orf82	0.282047868	0.388623477	0.43533254
C4orf34	4.236108296	2.959724102	2.075490432
C5orf38	2.118568019	3.252541727	2.570042221
C6orf48	6.593923999	5.909138584	2.673042098
CBLB	2.54518407	2.122823389	2.291347694
CCDC138	0.419424514	0.385597836	0.430872244
CCDC92	1.988802427	2.162093159	2.371967747
CCNA2	0.332440562	0.253578188	0.213349768
CCNB1	0.455416335	0.377863374	0.371344069
CCNB1IP1	2.260486552	2.830265363	3.520711353
CCNE1	0.343650087	0.350316184	0.419104484
CD68	4.250032949	2.314747981	3.959001885

CDC7	0.272959484	0.308105119	0.277675657
CDCA2	0.443962977	0.398038364	0.311930759
CDCA3	0.306614829	0.249790154	0.376917804
CDCA5	0.298787966	0.205763154	0.474861479
CDCA7	0.169231795	0.113149704	0.149774939
CDCA8	0.458009337	0.337054896	0.468274295
CDKN1C	2.653156246	2.911245812	5.001456828
CENPJ	0.310824975	0.328384339	0.419963352
CHAF1A	0.37843314	0.279655253	0.336662265
CHAF1B	0.385398925	0.299616787	0.301179025
CHEK1	0.372374773	0.331214111	0.386067868
CHRNA5	0.292676616	0.274383065	0.326725378
CKB	2.312561594	2.274518116	7.575166667
CPE	2.042128622	3.984208119	3.362317582
CRIP2	2.145092145	2.591143524	7.806921586
CRYAB	3.459757302	8.854932	4.33880944
CSE1L	0.394431066	0.441932337	0.271888069
CTSC	0.319021588	0.476264527	0.373915789
CYP4F3	4.368530719	3.849261788	9.630675504
DAPK1	2.574357992	5.796199587	2.406259316
DCC1	0.206451446	0.161108091	0.200721172
DCN	4.181060184	4.044213258	12.01697678
DDEF1	2.831304908	4.569974752	2.330241437
DDIT3	7.12143311	5.347949296	3.241077612
DDX39	0.331798817	0.340884494	0.429237287
DEPDC1	0.497440983	0.30696359	0.32884443
DHFR	0.281528978	0.278337826	0.29366923
DKFZp762E1312	0.400595072	0.342230576	0.329481242
DLG7	0.282026557	0.189652897	0.326482387
DNA2L	0.356982629	0.437391638	0.332038826
DNMT1	0.485424175	0.313246431	0.182510347
DONSON	0.453743753	0.430161673	0.391871865
DPYSL3	0.497744786	0.44701117	0.485819178
DUT	0.279152938	0.322002496	0.300012948
E2F2	0.230691242	0.202943728	0.244206305
EFHD2	0.44862624	0.358388707	0.461810762
ESCO2	0.313473636	0.267124278	0.227313281
ESPL1	0.438541867	0.326763295	0.477971948
EXO1	0.283496273	0.214511063	0.210743816
FAM134B	2.482458403	4.529869331	3.930706724
FAM43A	2.456029939	2.050305714	2.108117225
FAM81A	0.424131071	0.427681384	0.420442615
FAM83D	0.369533225	0.387770227	0.356804634
FANCI	0.362953568	0.255292986	0.27714391
FBLN1	2.900641315	1.987562154	3.547087241
FDPS	0.353597022	0.391265546	0.364043512
FEN1	0.334630816	0.253618062	0.206682803

FHOD3	0.213409863	0.286505481	0.287331079
FLRT3	3.018533191	3.492711406	2.096828365
FOXO3	2.205289859	2.559626347	2.270554737
FXYD3	2.034946132	4.247457281	2.345240468
GEMIN6	0.463668631	0.471112511	0.454838668
GINS2	0.265087383	0.136268471	0.199445581
GINS3	0.279368216	0.294180907	0.40781609
GINS4	0.34992914	0.254662123	0.397590206
GJB2	0.13778637	0.174157773	0.197887008
GPSM1	5.576670286	5.372485521	4.673408574
HELLS	0.403845101	0.337962329	0.28088811
HIST1H1C	3.986331976	4.583124921	4.955179276
HIST1H2BD	4.101156716	2.681156506	4.597808603
HIST2H2AA3	4.324044056	3.503177792	4.473779701
HIST2H2BE	6.792939944	7.133869903	3.042201085
HLA-E	2.167692279	2.215810949	2.634597676
HMGB3	0.267665767	0.354663089	0.331624044
HSD11B2	3.685418769	5.559761996	10.68222189
HSD17B8	2.875672637	3.086925414	2.062796161
HSPCAL3	0.493118902	0.423123036	0.161605784
HSPE1	0.390678428	0.469749214	0.41326361
IL1R2	0.225339229	0.182284339	0.406780327
INSIG1	0.381245218	0.439011773	0.334432531
KCNB1	3.512882407	4.672669362	4.27557549
KIAA0513	2.143071941	3.093698084	3.793709125
KIF11	0.378590319	0.370572868	0.441673691
KIF14	0.410810049	0.302687355	0.250165238
KIF2C	0.418667418	0.323762647	0.448261475
KLHDC9	2.450057928	3.207885709	3.623070326
KNTC1	0.424654967	0.443964634	0.413041207
KRT6B	0.442537237	0.355081321	0.228058829
LAMB2	2.170610365	3.145643766	5.262791822
LEMD1	8.298821835	3.005963377	4.393202458
LHPP	2.246935602	2.825880934	1.994855038
LMNB2	0.465656986	0.353158388	0.323818461
LOC153222	3.010405852	3.772841847	5.484720047
LOC554223	2.957286603	2.771217512	2.079672605
LOC649679	0.395338751	0.336174548	0.255523906
LOC729843	2.240952378	3.099275042	4.003816651
LOC91431	0.385916163	0.402322811	0.366862555
LOH11CR2A	4.141721251	3.288707215	3.883009111
LRP8	0.2119	0.161517705	0.11377922
LYRM5	2.30296076	2.739089349	2.116004462
MCM2	0.26377616	0.24873919	0.466051283
MCM3	0.228162447	0.293029488	0.280171156
MCM5	0.361122949	0.193870402	0.376173673
MCM7	0.188847528	0.221608234	0.400174601

METTL3	0.385454605	0.430111683	0.412052777
MLF1IP	0.346703192	0.316591946	0.424337986
MLKL	0.240197193	0.194387917	0.308172247
MME	2.339763099	5.536882134	6.618886123
MOSC1	0.283870844	0.258415955	0.415193499
MRTO4	0.477619318	0.421911841	0.343540806
MSH2	0.354612642	0.447705808	0.364330801
MSH6	0.328747507	0.367575223	0.387901586
MSX1	0.438567738	0.402120624	0.435636939
MT1G	0.159370727	0.079830027	0.373634708
MTBP	0.464321314	0.418207354	0.372819049
NCAPD3	0.364830202	0.363006721	0.319214047
NEIL3	0.400829876	0.316569365	0.340233684
NETO2	0.493065798	0.440610717	0.252902098
NFE2L1	2.134717132	3.637359064	3.102526832
NFIL3	2.604806284	3.162883243	2.88326635
NGFRAP1	2.125393091	3.154848577	2.155877241
NUP205	0.430884869	0.418984732	0.320644827
OIP5	0.394631063	0.310541835	0.434913387
PAQR4	0.403637533	0.245923791	0.325099965
PBK	0.383136451	0.435281366	0.240156165
PCNA	0.340403373	0.497534609	0.270480217
PDSS1	0.370073998	0.408470374	0.240810306
PDXP	0.431043682	0.456179259	0.263717857
PEX11G	3.143788641	2.79161817	2.225466822
PHLDA3	2.097599889	2.132099887	2.194606519
PKMYT1	0.473174259	0.267276819	0.326059317
PLCD1	3.103719883	2.893487038	2.714776962
PLEK2	0.385948815	0.13807659	0.253868122
PLK4	0.434079417	0.2573706	0.214727663
POLA2	0.32127739	0.236700726	0.270346496
POLD1	0.284141798	0.31499608	0.46657568
POLE2	0.198641319	0.149833983	0.214157747
POLQ	0.330791018	0.295203328	0.236022922
POLR3K	0.422497011	0.30762982	0.217136309
PPIL5	0.466143455	0.324018395	0.20799048
PPL	5.042821577	4.205350749	5.927355588
PRC1	0.352953919	0.279680521	0.490738832
PROS1	3.552265771	7.543219112	8.242123767
PRPF38A	0.490689798	0.475948808	0.408319042
RAD54B	0.367827083	0.432305457	0.409954771
RAD54L	0.247156598	0.214165498	0.294672815
RECQL4	0.428574832	0.406628583	0.43317599
RFC3	0.398641422	0.286821323	0.241213108
RFC4	0.476683584	0.377056541	0.342311821
RFC5	0.288510894	0.276698012	0.39454717
RIOK3	3.32215702	2.058417875	2.605796727

RNASEH2A	0.413995749	0.29363356	0.462917657
RRAGD	2.62423036	3.019393392	10.52803111
RRM2	0.293807027	0.177435017	0.167233833
SDCBP2	4.968487042	2.631710935	2.461071006
SERTAD4	0.18207468	0.193247708	0.273485421
SFPQ	0.481054817	0.459886633	0.439841148
SFRS2	0.390532688	0.424946817	0.316329318
SHCBP1	0.467173825	0.314352357	0.27257067
SIDT2	2.112281647	2.598423947	3.533338894
SLC25A10	0.366757353	0.413663231	0.385938871
SLC25A13	0.3253731	0.318201406	0.305206171
SLC45A3	0.324061764	0.251845416	0.347337365
SPC25	0.233682075	0.191563171	0.255831346
SRPK2	5.325304387	8.156428509	2.258578768
ST6GALNAC2	2.275729691	5.24415164	3.793785344
STAT2	3.442006522	3.321983458	3.884351895
SUV39H1	0.423203551	0.318140151	0.432156373
TACC3	0.408404594	0.26775563	0.406554646
TAF5	0.425569854	0.377222293	0.479227521
TERF1	3.482586178	2.574171086	1.991253458
TIGA1	3.35887033	3.656989703	4.303485007
TIMELESS	0.452567432	0.326599289	0.315361239
TINF2	2.706579645	2.261593028	2.452682168
TK1	0.342473588	0.199722221	0.367366618
TMC4	4.228104654	2.844461056	4.020721003
TMEM158	0.371872199	0.367480038	0.194658041
TMEM171	0.436850004	0.35272047	0.397406358
TMEM20	0.436129606	0.425239244	0.339034609
TNFRSF14	2.33571907	2.549978958	2.137889646
TRIP13	0.347862987	0.212376632	0.254101143
TTK	0.426424331	0.268271092	0.31057514
TUBA4A	0.412249298	0.392498538	0.299658729
TUBB2C	0.379517932	0.310280945	0.276899674
TUBB4Q	0.423296897	0.322564498	0.295043254
TXNIP	7.639216083	7.310636174	7.211355318
TYMS	0.306860622	0.338928211	0.390962898
UHRF1	0.227961697	0.169696234	0.176490453
VAMP5	2.155872871	2.608012186	2.337641787
VRK1	0.423989177	0.313617272	0.338598343
WDHD1	0.453924776	0.494572487	0.474699598
WDR79	0.364409741	0.36745668	0.427644086
WIPI1	2.856431861	3.01597785	2.139754972
XPC	2.121985007	2.974242792	2.38238061
YPEL5	2.053624187	2.837300869	3.323701875
ZBTB43	2.074065723	3.15142501	2.718191208
ZNF467	2.339376189	2.293554436	9.782257743

Supplementary Table 2: Change of protein expressions between HRD and HR-Intact cells

Gene Symbol	Fold change of protein expression (log2; HRD-HRI)
HIST2H2BE	2.556334151
CRIP2	1.39199774
HIST1H1C	0.964876083
CKB	0.933599789
HSD17B8	0.869685769
SRPK2	0.825821573
CDKN1C	0.622791483
TMC4	0.482100578
BBOX1	0.477039883
ATP10B	0.370033598
ADM	0.304107288
BTG1	0.304107288
ZNF467	0.304107288
FOXO3	0.283759237
LAMB2	0.283048896
NFIL3	0.266214297
HLA-E	0.261664324
STAT2	0.246909199
CCDC92	0.235994459
ALDH6A1	0.219494635
TINF2	0.20988541
FAM134B	0.204056964
WIPI1	0.204056964
RIOK3	0.173404758
XPC	0.160120276
ARSD	0.159716707
SDCBP2	0.149647189
ALDH3B1	0.100518239
TNFRSF14	0.066606971
VAMP5	0.066606971
KIAA0513	0.058775178
CD68	0.054910808
PLCD1	0.054910808
ST6GALNAC2	0.041966278
CBLB	0.035595689
RFC4	-0.006349747
TMEM158	-0.011627835
LRP8	-0.017292496
DONSON	-0.021600071
ASF1B	-0.033199971

MT1G	-0.050323523
TUBB4Q	-0.053956643
CCNE1	-0.083270614
POLD1	-0.090682089
GINS4	-0.094387468
PLEK2	-0.117094537
POLQ	-0.126312198
RNASEH2A	-0.12809325
PRC1	-0.131410255
MSH6	-0.140207518
TYMS	-0.174623925
FANCI	-0.194487889
WDHD1	-0.19879118
BLM	-0.208861963
C11orf82	-0.218339806
RFC3	-0.29024922
DPYSL3	-0.317597756
C14orf145	-0.365709844
ASPM	-0.444256783
PDXP	-0.44573542
CDCA2	-0.455143465
MRTO4	-0.51528056
DNMT1	-0.555028316
SLC25A13	-0.566738014
KIF14	-0.596530669
CCNA2	-0.648020185
CCNB1	-0.759072146
MCM5	-0.798476624
KIF2C	-0.836327094
ANLN	-0.965423785
MSH2	-0.966949371
CTSC	-1.001087875
C10orf119	-1.129001934
NUP205	-1.235251204
TUBA4A	-1.307098927
HMGB3	-1.32621119
LMNB2	-1.826436807
FDPS	-1.935751084

Supplementary Table 3: Target sequences of shRNAs/siRNAs

shRNA	
<i>BRCA1</i> #1	MISSION® shRNA Lentiviral Transduction Particles Sequence #4 CCGGGCCACCTAATTGTACTGAATCTCGAGATTCACTGAGATTGGCTTTG
<i>BRCA1</i> #2	MISSION® shRNA Lentiviral Transduction Particles Sequence #5 CCGGCCTACAAGAAAGTACGAGATCTCGAGATCTGACTTCTTAGGCTTTG
<i>BRIT1</i> #1	MISSION® shRNA Lentiviral Transduction Particles Sequence #1 CCGGCCATGTGTTGTGGTTCTAACCTCGAGTTAAGAACACACATGGCTTTG
<i>BRIT1</i> #2	MISSION® shRNA Lentiviral Transduction Particles Sequence #2 CCGGCAATGGAGAAGAGATTACAACACTCGAGTTGAATCTCTCCATTGCTTTG
<i>RAD51</i> #1	MISSION® shRNA Lentiviral Transduction Particles Sequence #1 CCGGCTGAAGCTATGTCGCCATTCTCGAGAACATGGCACATAGCTCAGCTTTG
<i>RAD51</i> #2	MISSION® shRNA Lentiviral Transduction Particles Sequence #2 CCGGCGGTCAAGAGATCATACAGATTCTCGAGAACATGGCACATAGCTCAGCTTTG
<i>PTEN</i> #1	MISSION® shRNA Lentiviral Transduction Particles Sequence #1 CCGGAGGCGCTATGTATTATTCTCGAGATAATAACACATAGCGCTTTT
<i>PTEN</i> #2	MISSION® shRNA Lentiviral Transduction Particles Sequence #2 CCGGCCACAGCTAGAACTTATCAAACACTCGAGTTGATAAGTTCTAGCTGTGGTTTT
<i>ATM</i> #1	MISSION® shRNA Lentiviral Transduction Particles Sequence #1 CCGGTGATGGCTTAAGAACATCTCTCGAGAGATGTTCTTAAGACCACATTTG
<i>ATM</i> #2	MISSION® shRNA Lentiviral Transduction Particles Sequence #3 CCGGGCCTCCAATTCTCACAGTAACACTCGAGTTACTGTGAAGAACAGCTTTG
<i>ATR</i> #1	MISSION® shRNA Lentiviral Transduction Particles Sequence #3 CCGGAATGCATTGGTATGAATCTGCTCGAGCAGATTACCAATGCATTTTG
<i>ATR</i> #2	MISSION® shRNA Lentiviral Transduction Particles Sequence #4 CCGGCTGTGGTTGTATCTGTTCAATCTCGAGATTGAACAGATAACACAGCTTTG
<i>CHK1</i> #1	MISSION® shRNA Lentiviral Transduction Particles Sequence #3 CCGGGTGGTTATCTGCATGGTATTCTCGAGAACACATGCAGATAAACCAACTTTT
<i>CHK1</i> #2	MISSION® shRNA Lentiviral Transduction Particles Sequence #4

	CCGGGTAAACAGTGCTTCTAGTGAACTCGAGTCACTAGAACGCAGTTACTTTT
<i>CHK2#1</i>	MISSION® shRNA Lentiviral Transduction Particles Sequence #1 CCGGGAACAGATAAAATACCGAACATCTCGAGATGTTCGGTATTATCTGTTCTTTT
<i>CHK2#2</i>	MISSION® shRNA Lentiviral Transduction Particles Sequence #2 CCGGACGATGCCAAACTCCAGCCAGCTCGAGCTGGCTGGAGTTGGCATCGTTTTT
<i>53BP1#1</i>	MISSION® shRNA Lentiviral Transduction Particles Sequence #1 CCGGGATACTTGGTCTTACTGGTTCTCGAGAAACCAGTAAGACCAAGTATCTTTT
<i>53BP1#2</i>	MISSION® shRNA Lentiviral Transduction Particles Sequence #2 CCGGCCAGTGTGATTAGTATTGATTCTCGAGAATCAACTAATCACACTGGTTTTT
<i>BRCA2#1</i>	MISSION® shRNA Lentiviral Transduction Particles Sequence #2 CCGGGCCTGAATAATCACAGGCAACTCGAGTTGCCTGTGATTATTCAAGGCTTTG
siRNA	
<i>ZNF668</i>	Target Sequence: GUGCAGCGACUUGCGCAAUU Target Sequence: AAGCCAUACCACUGCGAGAUU
<i>TTK</i>	Target Sequence: GAUAAGAUCAUCCGACUUU (J-004105-09) Target Sequence: GCAAUACCUUGGAUGAUUA (J-004105-10) Target Sequence: CCAGUUAACCUUCUAAAUA (J-004105-11) Target Sequence: GAUAGUUGAUGGAAUGC (J-004105-12)
<i>BRCA1</i>	Target Sequence: CAACAUGCCCCACAGAUCAA (J-003461-09) Target Sequence: CCAAAGCGAGCAAGAGAAU (J-003461-10) Target Sequence: UGAUAAAGCUCCAGCAGGA (J-003461-11) Target Sequence: GAAGGAGCUUCAUCAUUC (J-003461-12)

Supplementary Methods:

Proteome profiling

For proteome analysis, cells were grown in RPMI 1640 supplemented with ¹³C-lysine and 10% dialyzed FBS¹. Cells were lysed in 1 ml of PBS containing the detergent octyl-glucoside (OG) (1% w/v) and protease inhibitors (complete protease inhibitor cocktail, Roche Diagnostics), followed by sonication and centrifugation at 20,000×g with collection of the supernatant. Two mg of whole cell lysate were reduced in DTT and alkylated with iodoacetamide before fractionation with reverse-phase chromatography. Individual fractions were digested in-solution with trypsin and combined into 24 pools based on chromatographic features; pools were analyzed individually on an LTQ-Orbitrap mass spectrometer (Thermo Scientific). Mass spectrometry data were processed by CPAS and spectra searched against a composite database of IPI human (v3.57) and IPI bovine (v3.43). Significance of peptide and protein matches was estimated with PeptideProphet and ProteinProphet. Peptides with a minimum PeptideProphet of 0.05 were submitted to ProteinProphet with a 5% maximum error rate and any unlabeled peptides with bovine homology were discarded².

Antibodies

ATR (SC-1887, 1:500), CHK1 (SC-8408, 1:500) antibodies were purchased from Santa Cruz. ATM (#2873, 1:1000), CHK2 (2662, 1:1000), 53BP1 (4937, 1:1000), PTEN (9559, 1:1000) and vinculin (4650, 1:1000) antibodies were from Cell Signaling. BRIT1 antibody was generated as previously described³ (1:1000). RAD51 (PC130) antibody was from Millipore Corp.

Supplementary References

1. Taguchi, A., *et al.* Lung cancer signatures in plasma based on proteome profiling of mouse tumor models. *Cancer cell* **20**, 289-299 (2011).
2. Faca, V.M., *et al.* Proteomic analysis of ovarian cancer cells reveals dynamic processes of protein secretion and shedding of extra-cellular domains. *PloS one* **3**, e2425 (2008).
3. Mills, G.B., *et al.* Expression of TTK, a novel human protein kinase, is associated with cell proliferation. *The Journal of biological chemistry* **267**, 16000-16006 (1992).